

Comment on “Structural analysis of mylonitic rocks in the Cougar Creek Complex, Oregon–Idaho using the porphyroclast hyperbolic distribution method, and potential use of SC' -type extensional shear bands as quantitative vorticity indicators”

Yadong Zheng^{a,*}, Tao Wang^b, Jinjiang Zhang^a

^aThe Key Laboratory of Orogenic Belts and Crustal Evolution, Ministry of Education, School of Earth and Space Sciences, Peking University, Beijing 100871, China

^bInstitute of Geology, Chinese Academy of Geological Sciences, Beijing 100037, China

ARTICLE INFO

Article history:

Received 12 August 2008

Received in revised form

21 January 2009

Accepted 25 January 2009

Available online 5 February 2009

Keywords:

Shear bands

Vorticity indicators

Maximum-effective-moment criterion

1. Introduction

The position of shear bands in the associated flow field is poorly understood and differently described in the literature. Two major opinions on the issue reviewed by Kurz and Northrup (2008) are: 1) one believes that their orientations were initially coincidental with the directions of maximum shear strain rate, with synthetic and antithetic shear bands parallel to the acute bisector (AB) and the obtuse bisector (OB) of the eigenvectors, respectively (e.g. Simpson and De Paor, 1993); 2) another suggests that they were parallel to the inclined or unstable eigenvector (e.g. Bobyarchick, 1986). A new idea however that shear bands are parallel to maximum-effective-moment (MEM) orientations (Zheng et al., 2004) was overlooked. Kurz and Northrup well documented the shear bands in mylonitic rocks of the Cougar Creek Complex in terms of rose diagrams of their orientations combined with PHD vorticity to illustrate the geometric relationships of their orientations and the eigenvectors (their Fig. 4a–e), and provide an opportunity to explore the role of them in vorticity analysis. Kurz and Northrup believed that

although extensional SC' -type shear bands are inclined at an angle less than AB and OB with the obtuse angle in the contractional direction, the shear bands initially formed parallel to AB and OB. They referred that the shear bands tend to rotate towards the flow with progressive deformation. Is this explanation reasonable and acceptable?

2. 109.4° – theoretical angle between the conjugate shear bands

As early, White (1979), for the first time, reported that conjugate shear bands in mylonite have $\sim 110^\circ$ in the contractional direction. The theoretical angle of 109.4° and practical angles of $110 \pm 10^\circ$ (Fig. 1) have been confirmed by Zheng et al. (2004), and observations of the conjugate angle are increasingly appeared in the literature (e.g. Neves et al., 2005; Marshak et al., 2006; Zheng et al., 2006; Guo et al., 2006; Yang et al., 2007; King et al., 2008). The excellent work on experimentally ductile deformed quartz single crystals by Vernooij et al. (2006) reveals that conjugated shear bands have an angle of 109° or 110° when the crystal is uniaxially compressed parallel to the crystallographic c -axis and its bulk strain up to $\sim 26\%$. If the shear bands formed initially parallel to the orientations of maximum angular strain rate, as Kurz and Northrup suggested, and then rotated towards the flow plane, the least bulk strain needed would be 31%, which is obviously higher than $\sim 26\%$. The experiment demonstrates that the shear bands are parallel to MEM-orientations and that the angle of 110° in the σ_1 -direction does not increase with progressive strain at least the related bulk strain is up to $\sim 26\%$. Conjugate shear bands in Figs. 4a, d and 8 provided by Kurz and Northrup show that the conjugate angles are 116° and 107° for their Fig. 4a and d, and 108° and 98° for their Fig. 8a and b, respectively. All of them fall into the range predicted by the MEM criterion (Fig. 1). The orientations of shear bands therefore are most likely controlled by MEM-orientations rather than those of maximum shear strain rate. There is no need to resort to rotation of shear bands to solve the conjugate-angle issue.

DOI of original article: 10.1016/j.jsg.2008.04.003.

* Corresponding author.

E-mail address: ydzheng@pku.edu.cn (Y. Zheng).

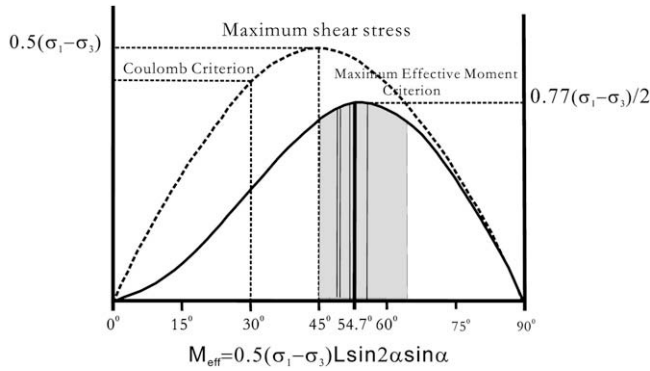


Fig. 1. The maximum-effective-moment criterion (MEMC) with the shadow area covering all the data available and vertical lines showing the four angles between conjugate shear bands reported by Kurz and Northrup (2008): $(\sigma_1 - \sigma_3)$ – yield strength of the material; α – the angle between σ_1 and the normal to shear bands/zones; L – unit length.

3. Shear bands as quantitative vorticity indicators

When the limiting assumptions made are: 1) homogeneous bulk deformation; 2) no volume change; plane deformation, and if only the ratio of the vorticity and strain rate remains fixed, W_k can be given by the relationship $W_k = \sin 2\xi$ where ξ is the angle between σ_1 or the minimum instantaneous incremental stretching axis (ISA₃) and the normal to the shear zone (Weijermars, 1998). Based on the relationships between shear bands, major principal stress axis (σ_1) and W_k , W_k can be estimated. Taking Sample CC-6-6-2 for example, the mean conjugate angle is 107°, the angle between the bisector and normal to the shear zone is 7°, and corresponding W_k is given by $\sin(2 \times 7^\circ)$, that is 0.24 (Fig. 2). W_k values inferred from similar way for their Fig. 4a–d are 0.50, 0.53, 0.50, 0.24, 0.56 and 0.63, which are much higher than the PHD values 0.26–0.37 given by Kurz and Northrup, but highly consistent with those given by critical shape factor B^* analysis except for 0.24 (Table 1).

The PHD values are based on trail-geometry. The problem is not all that σ -type inclined “downstream” porphyroclasts with asymmetric tails attached to their broad sides are back-rotation grains. Some of them regarded as back-rotating grains are actually forward-rotating ones, for forward rotation of a porphyroclast with long axis oriented antithetic to the flow only inhibits, but does not prevent σ -tails to growth (Forte and Bailey, 2007). The forward-rotating grains may have similar geometry with those back-rotating grains when their forward-rotation rate is less than dynamic recrystallization rate. Since some forward-rotating grains are inevitably treated as back-rotation ones and, in the result, coaxial component in shear zones tends to be overestimated. The issue can be solved by treating all data as tailless porphyroclasts on PHD plots or rigid grain net (RGN) proposed by Jessup et al. (2007), and all data provided by Kurz and Northrup are treated here in this way to re-estimated W_k of the related shear zones in terms of $W_k^{B^*}$ (Table 1). The results are highly consistent with our $C' - \sigma_1$ values except for 0.24 in Sample CC-6-6-2 (Fig. 2) and another W_k in Sample CC-5-27-4 (Table 1). $C' - \sigma_1$ analysis is also used for data of the low strained rocks in their Fig. 8 and obtained W_k of 0.21 and 0.03 (Table 1), which imply much more coaxial component in low strained domains of the related shear zones.

Since spaced shear bands usually transect and displace the penetrative mylonitic foliation and therefore the related W_k represents the non-coaxiality when the shear bands formed. If the ratio of the vorticity and strain rate remains fixed, the W_k may be close to PHD values. If the ratio of the vorticity and strain rate changed, the W_k derived from $C' - \sigma_1$ analysis may only record the non-coaxiality when the shear bands formed, relatively later episode of progressive deformation. It is not realistic to expect a unique W_k throughout a deformation event. W_k values inferred from shear band orientations are usually less than PHD or RGN values, for spaced shear bands tend to form later than penetrative mylonitic fabrics and displacement field or deformation partitioning would increase the relative contribution of coaxial component in shear zones (e.g. Tikoff and Teysier, 1994; Zheng and Wang, 2005).

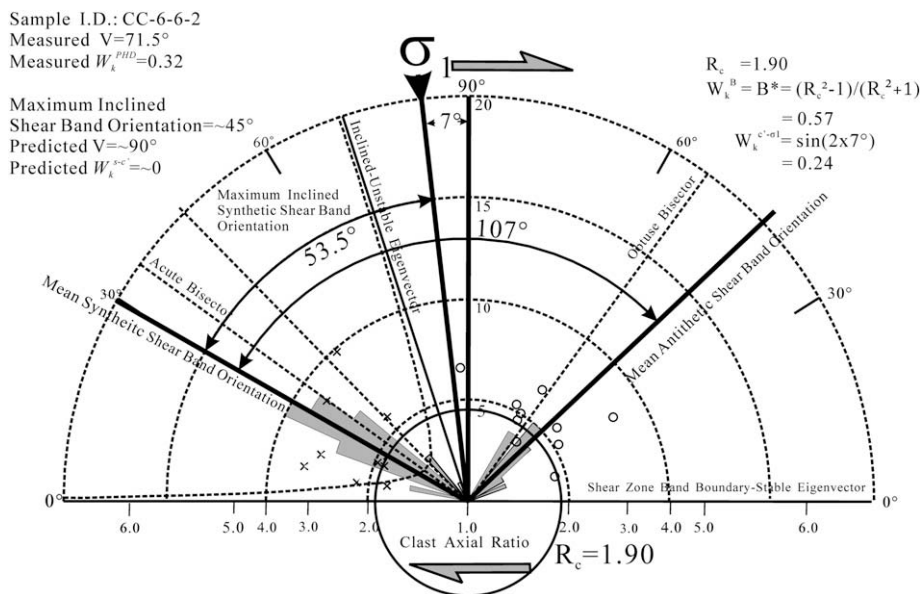


Fig. 2. Re-estimated W_k based on Fig. 4d of Kurz and Northrup (2008): $W_k^{PHD} - W_k$ given by Kurz and Northrup (2008); $W_k^{B^*} - W_k$ from PHD analysis with treating all data as tailless porphyroclasts. Critical shape factor ($B^* = (R_c^2 - 1)/(R_c^2 + 1)$), where R_c represents critical aspect ratio of porphyroclasts; $W_k^{C' - \sigma_1} - W_k$ given by $\sin 2\xi$, where ξ is the angle between σ_1 axis and normal to the shear zone and σ_1 orientation is given by the obtuse bisector of conjugate shear bands or half the theoretical conjugate angle 110°.

Table 1Comparison between original and re-estimated W_k values.

Sample	W_k^{PHD} (Kurz and Northrup, 2008)	W_k^{SC} (Kurz and Northrup, 2008)	W_k^{B*}	$W_k^{C-\sigma_1} - 1$	$W_k^{C-\sigma_1} - 2$
CC-5-27-4	0.31	0.31	0.46	0.50	0.03
CC-6-9-1	0.36	0.41	0.56	0.53	
CC-6-9-2	0.26	0.50	0.63	0.50	
CC-6-6-2	0.32	0.00	0.57	0.24	
CC-7-9-1	0.37	0.24	0.60	0.56	
CC-6-15-1	0.32			0.63	
CC-6-30-1		0.50		0.21	
CC-6-4-1		0.17		0.03	

4. Conclusions

SC'-type shear bands described by Kurz and Northrup (2008) are most likely controlled by MEM-orientations rather than those of maximum shear strain rate that they suggest. Since the orientations of shear bands are theoretically at angle of 54.7° and practically at angles $55 \pm 10^\circ$ with σ_1 - or ISA_3 -axis, SC'-type shear bands may serve as reliable quantitative vorticity indicators for homogeneous two-dimensional flow by means of the formula of $W_k = \sin 2\xi$, where ξ is the angle between σ_1 or ISA_3 and the normal to shear zone boundary. W_k values inferred from shear bands are not necessary to be consistent with those from PHD or RGN analysis, which depends on stability of the related flow. Since spaced shear bands generally formed later than penetrative mylonitic fabrics and displacement or strain partitioning during progressive non-coaxial flow are likely to happen, the related W_k numbers tend to be much less than their PHD counterparts.

Acknowledgments

The authors are financially supported by NNSFC (Grant No. 90714006).

References

- Bobyarchick, A.R., 1986. The eigenvalues of steady state flow in Mohr space. *Tectonophysics* 122, 35–51.
- Forte, A.M., Bailey, C.M., 2007. Testing the utility of the porphyroclast hyperbolic distribution method of kinematic vorticity analysis. *Journal of Structural Geology* 29, 983–1001.
- Guo, Z.J., Shi, H.Y., Zhang, Z.C., Zhang, J.J., 2006. The tectonic evolution of south Tianshan paleo-oceanic crust inferred from the spreading structures and Ar–Ar dating of the Hongliuhe ophiolite, NW China. *Acta Petrologica Sinica* 22, 95–102.
- Jessup, M.J., Law, R.D., Frassi, C., 2007. The rigid Grain Net (RGN): an alternative method for estimating mean kinematic vorticity number (W_m). *Journal of Structural Geology* 29, 411–421.
- King, D.S., Klepeis, K.A., Goldstein, A.G., Gehrels, G.E., Clarke, G.L., 2008. The initiation and evolution of the transpressional Straight River shear zone, central Fiordland, New Zealand. *Journal of Structural Geology* 30, 410–430.
- Kurz, G.A., Northrup, C.J., 2008. Structural analysis of mylonitic rocks in the Cougar Creek Complex, Oregon–Idaho using the porphyroclast hyperbolic method, and potential use of SC'-type extensional shear bands as quantitative vorticity indicators. *Journal of Structural Geology* 30, 1005–1012.
- Marshak, S., Alkmim, F.F., Whittington, A., Pedrosa-Soares, A.C., 2006. Extensional collapse in the Neoproterozoic Aracuaí orogen, eastern Brazil: a setting for reactivation of asymmetric crenulation cleavage. *Journal of Structural Geology* 28, 129–147.
- Neves, S.P., de Silva, J.M.R., Mariano, G., 2005. Oblique lineations in orthogneisses and supracrustal rocks: vertical partitioning of strain in a hot crust (eastern Borborema Province, NE Brazil). *Journal of Structural Geology* 27, 1513–1527.
- Simpson, C., De Paor, D.G., 1993. Strain and kinematic analysis in general shear zones. *Journal of Structural Geology* 15, 1–20.
- Tikoff, B., Teyssier, C., 1994. Strain modeling of displacement field partitioning in transpressional orogens. *Journal of Structural Geology* 16, 1579–1588.
- Vernooij, M.G.C., Kunze, K., den Brok, B., 2006. 'Brittle' shear zones in experimentally deformed quartz single crystals. *Journal of Structural Geology* 28, 1292–1306.
- Weijermars, R., 1998. Taylor-mill analogues for patterns of flow and deformation in rocks. *Journal of Structural Geology* 20, 77–92.
- White, S.H., 1979. Large strain deformation: report on a Tectonic Studies Group discussion meeting held at Imperial College, London on 14 November 1979. *Journal of Structural Geology* 1, 333–339.
- Yang, T.N., Wang, Y., Li, J.Y., Sun, G.H., 2007. Vertical and horizontal strain partitioning of the Central Tianshan (NW China): evidence from structures and Ar–40/Ar–39 geochronology. *Journal of Structural Geology* 29, 1605–1621.
- Zheng, Y., Wang, T., Ma, M., Davis, G.A., 2004. Maximum effective moment criterion and the origin of low-angle normal faults. *Journal of Structural Geology* 26, 271–285.
- Zheng, Y.D., Wang, T., 2005. Kinematics and dynamics of the Mesozoic orogeny and late-orogenic extensional collapse in the Sino-Mongolian border areas. *Science in China (Series D – Earth Sciences)* 48, 849–862.
- Zheng, Y.D., Wang, T., Wang, X.S., 2006. The maximum effective moment criterion (MEMC) and its implications in structural geology. *Acta Geologica Sinica (English Edition)* 80, 70–78.